American Journal of Nanosciences
2020; 6(4): 34-44
http://www.sciencepublishinggroup.com/j/ajn
doi: 10.11648/j.ajn.20200604.12
ISSN: 2575-484X (Print); ISSN: 2575-4858 (Online)

Expression Analysis of the *Candida albicans KEX2, SAP1, CDR1* and *LIP1*genes Influenced by Biosynthesized Silver Nanoparticles

Muhsen Mohamed Faraj, Kamil Mutashar Al-Jobori

Institute of Genetic Engineering and Biotechnology for Postgraduate Studies, University of Baghdad, Baghdad, Iraq

Email address:
kamilaljobori@yahoo.com (K. M. Al-Jobori)

To cite this article:
Muhsen Mohamed Faraj, Kamil Mutashar Al-Jobori. Expression Analysis of the *Candida albicans KEX2, SAP1, CDR1* and *LIP1*genes Influenced by Biosynthesized Silver Nanoparticles. *American Journal of Nanosciences*. Vol. 6, No. 4, 2020, pp. 34-44.
doi: 10.11648/j.ajn.20200604.12

Received: October 28, 2020; **Accepted**: November 26, 2020; **Published**: January 18, 2021

Abstract: Present investigation deals with the synthesis of silver nanoparticles (AgNPs) from *Lycopersicon esculentum* L. through simple and eco-friendly method and validation the capacity of nanoparticles to inhibit the virulence gene expression in *Candida albicans*. The nanoparticles thus obtained from *Lycopersicon esculentum* L. have been analysed and characterised by Scanning Electron Microscopy (SEM), UV-Vis spectrophotometer, X-ray diffraction (XRD) and Fourier Transform Infra-red Spectroscopy (FTIR) techniques. The average diameter of the AgNPs, whose morphology has been determined by SEM, was found to be 9.58 to 72.69 nm. The UV-vis spectrophotometer show peak located of silver nanoparticles at 340 nm. X-ray diffraction analysis also showed functional structure and pattern of silver nanoparticles. The FT-IR spectra indicated the role of different functional groups of reducing agent and silver nanoparticles. AgNPs at concentrations of 15 and 25% significantly downed expression of *Sap1, LIP1* and *Kex2*, but had no effect on the expression of *CDR1* gene. The findings of current study showed that tomato extract could be used as a green chemistry approach to produce AgNPs. It downed expression of *Sap1, LIP1* and *Kex2* genes, whereas had no effect on the expression of *CDR1* gene, that it appears needs higher concentrations of AgNPs to inhibit its gene expression.

Keywords: Lycopersicon Esculentum, Agnanoparticles, *Candida albicans*, Virulence Genes Sap1, LIP1, Kex2, CDR1

1. Introduction

The human pathogen *C. albicans* is the fourth leading cause of nosocomial bloodstream infections. Although this pathogen has been associated with a high mortality rate, it is described as a harmless commensal of the normal human microflora residing on both skin and mucosal surfaces. Currently, approximately 5 million fungal species have been classified, of which an estimated 300 are capable of establishing disease within a mammalian host [1]. Amongst these *Candida* pathogens, *C. albicans* is the species mostly common associated with human infection [2]. *It* can cause two major types of infections in humans: superficial infections of the skin, such as oral or vaginal candidiasis, and life-threatening systemic infections [3]. The ability of some fungal species to cause disease is due to various virulence factors which help with fungal survival and retrieve in the host resulting in tissue damage and disease [4]. The pathogenicity of the *Candida* species is attributed to critical virulence factors, such as cellular morphogenesis, cell-surface adhesion, phenotypic switching, biofilm formation, antifungal drug resistance, and secretion of hydrolytic enzymes such as secreted aspartyl proteases (*SAP*) and phospholipases and lipase enzymes [5].

Candida albicans is not only able to develop resistance to antifungal drugs, it also has the capability of adapt to various environments, furthermore, many antifungal drugs can cause severe side effects after prolonged treatment. In combat against the fungal infections, three main defects can be considered for some antifungal drugs: first, they operate in a limited range, second they can negatively react with different types of antifungal agents, and third they can make the microorganisms resistant [6].

Metal nanoparticles have been produced chemically, physically, and recently, biologically. However, the

conventional physical and chemical reduction methods continue to be extensively used for nanoparticle production, use of toxic chemicals, high energy consumption, as well as high production costs remain as the major challenges for the industry. Developing a green chemistry approach as nontoxic, eco-friendly, sustainable and relatively cost-effective method for nanoparticle production is a growing research interest [7]. NPs are particles having the size range of 100 nm and are clusters of atoms. Nanotechnology is expected to play a vital role in various disciplines and is becoming the most innovative scientific field. Nanotechnology mainly concerns with the synthesis of NPs of variable sizes, shapes, chemical compositions and the potential use for human benefits [8]. In general, nanoparticle structures consist of three layers: (i) core, (ii) shell, and (iii) surface [9]. Nanoparticles exhibit unusual physical, chemical and biological activity due to their small sizes and they are applied in various disciplines including engineering agriculture, electronics, automotive, information and communication technologies, energy, textile, construction medical, and household products [10, 11].

To evaluate the synthesized nanomaterials, many analytical techniques have been used, including Ultraviolet Visible spectroscopy (UV-vis spectroscopy), X-Ray Diffractometry (XRD), Fourier Transform Infrared spectroscopy (FTIR), X-ray Photoelectron Spectroscopy (XPS), Dynamic Light Scattering (DLS), Scanning Electron Microscopy (SEM), Transmission Electron Microscopy (TEM), Atomic Force Microscopy (AFM), and so on [12, 13]. Due to their unique properties, AgNPs have been used extensively in various applications [14]. There are three well-defined mechanisms have been proposed: (i) cell wall and membrane damage, (ii) intracellular penetration and damage, and (iii) oxidative stress [15]. Silver nanoparticles synthesized by green chemistry offer a novel and potential alternative to chemically synthesized nanoparticles. [16]. Nanosilver, due to its small particle size and enormous specific surface area, facilitates more rapid dissolution of ions than the equivalent bulk material; potentially leading to increased toxicity of nanosilver [17]. omato are edible and abundantly available, it is well known that tomatoes are rich in antioxidants, such as lycopene, phenolics, flavonoids phytoalexins, protease inhibitors, glycoalkaloids and ascorbic acid. These metabolites protect against adverse effects of hosts of predators including fungi, bacteria, viruses, and insects. In addition, these antioxidants could act as effective reducing agents during the synthesis of nanoparticles, and thus, will allow to the biosynthesis process for nanoparticle production. Hence, the present study deals with:

2. Materials and Methods

2.1. Clinical Specimens Collection

During the period between early December 2018 to the end May 2019, a total of 110 clinical specimens were collected from patients hospitalized in Baghdad city (Kamal AL-Samarea and AL-Karkh hospitals), and General Tikrit hospital aged from 1-71 years as follows: Different sources was collected from mouth, vginal swabs the sputum specimens were collected in sterile containers. The samples were taken by sterile swabs with a transport medium. All specimens were collected using clean sterile containers and the transport swabs were damped with normal saline, to be transported to the laboratory immediately.

2.2. Isolation of Candida Albucans

Clinical samples were transported quickly to the bacteriological laboratory of each hospital under aseptic conditions. Each specimen was streaked on a selective media using a direct method of inoculation to investigate the presence of *C. albucans*, typical CHROM agar S. D. A it was incubated under aerobic conditions for 24 hrs at 37°C [18].

2.3. Preparation of Tomato Fruit Extract

Tomato *(Lycopersicum esculentum* Mill) plants were grown in a greenhouse located at College of Sciences of Agriculture Engineering, University of Bagdad. The plants were kept in the 4 ˚C temperature. Tomato fruits were harvested at the light red stage of ripeness. Calyces were removed and whole fruits were thoroughly washed and homogenized using a hand-held blender for 2 min. To prevent compositional changes, the homogenized extract was clarified by repeated (3×) centrifugations for 15 minutes at 15,000 and stored at 20°C for further experiments.

2.4. Preparation of mM $AgNO_3$ Solutions

One milimolar solution of $AgNO_3$ 0.034g was prepared by dissolving in 100ml deionized water (DIW), and stored in coloured bottle in cool and dry place.

2.5. Green Synthesis of AgNPs and Characterization

Ten ml of aqueous fruit extract at 20% concentration was added into 20ml aqueous solution of 2 mM $AgNO_3$ aqueous solution at pH9 and temperature 100°C into 170 ml of deionized water for reduction into Ag^+ ions at room temperature [19]. The reaction mixture was optimized at different controlled conditions for the green synthesis of AgNPs. The bioreduction of Ag+ ions was monitored using UV-vis spectrophotometer ((Systronics double beam spectrophotometer 2202, India) between the range of 350nm and 550nm). Analysis of size andmorphology ofAgNPs was performed by Scanning electron microscope SEM (ZEISS-EVO MA 15, Japan). The purified crystalline Ag NPs were examined by X-ray diffraction XRD analysis, The measurements were performed with a Philips PW 1140/90 diffractometer (Philips Analytical, Almelo, The Netherlands) operating at a voltage of 40 kV and a current of 30 mA with Cu Kα radiation (λ=1.54060 Å). The scanning was executed in a region of 0.2θ from 10° to 90° at 0.01°/min. Fourier Transform Infrared Spectroscopy (FT-IR), Shemadzu, (Germany), spectrum was used to calculate the various functional groups present in AgNPs, The infrared spectra for the green synthesized AgNPs were attained for the identification of functional groups in a (Perkin-Elmer 1725x, Japan) spectrophotometer by employing

KBr pellet technique operating at a resolution accuracy of 4 cm^{-1} under ambient condition.

3. Gene Expression

3.1. Extraction, Measurement of RNA and cDNA Synthesis

RNA was extracted with the TRIzol kit according to the manufacturer's recommendations. The extracted RNA was quantified (ng/µL) in a Nanodrop 2000 spectrophotometer (Thermo Fisher Scientific). Absorbance ratios (260/280) of ~2.0 indicate the degree of purity necessary for good performance of the subsequent reactions. The RNA was transcribed to complementary DNA (cDNA) using the WizScript™ RT FDmix Kit according to the manufacturer's instructions.

3.2. Quantitative Real Time PCR (qRT–PCR)

To confirm the expression levels of the target genes, the results were normalized using reference gene *ACT1*, quantitative real time qRT-PCR SYBR Green assay was used. The primers sequences sets for target genes *SAP1, CDR1, LIP1*, and reference gene *ACT1*were used as described previously (Table 1). While The sequence of the primer set of *KEX2* gene was designed by using Primer1 (Primer-BLAST, NCBI). They were provided in a lyophilized form and dissolved in sterile nuclease-free water to give a final concentration of 100 µM /µl and stored in the deep freezer until use. This process was undertaken on the qPCR Master Mix kit using SYBR green fluorescent dye. Q RT-PCR was performed using Real-time PCR System with qPCR software.

Table 1. *The primers and their sequences used in the real-time-PCR.*

Primer	Sequence (5′→3′ direction)	Product length (Pb)	Reference
*Gene 1*SAP1		224	Correia *et al.,* 2010
Forward	TGAGGCTGCTGGTGATTATG		
Reverse	TGCCAACAGCTTTGAGAGA		
Gene 2 CDR1		142	Monroy-Pérez *et al.,* 2016
Forward	AAGATGTCGTCGCAAGATGAATC		
Reverse	GAGTGAAAGTTCTGGCTAAATTCTGA		
Gene 3 LIP1		58	Nailis *et al*., 2010
Forward	AGCCCAACCAGAAGCTAATGAA		
Reverse	TGATGCAAAAGTCGCCATGT		
*Gene 4*KEX2		127	In this study
Forward	CTTGCCAGATTGTCCACTTTTG		
Reverse	GTAAATCAACCACTACAACCAGC		
Gene 5 Reference Gene ACT1		186	Correia *et al.*, 2010
Forward	TGCTGAACGTATGCAAAAGG		
Reverse	TGAACAATGGATGGACCAGA		

The reaction mixture (25 µl) contained 12.5 µl of qPCR Master Mix, 1 µl of each primer, 3µl of template cDNA and 7.5 µl of nuclease-free water. Amplifications were performed using the following cycling profile: For *SAP1*and *ACT1*genes an initial activation step (95°C for 5 min) followed by 40 cycles of denaturation at 95°C for 15 s, annealing at 58°C for 30 s, and extension at 72°C for 20 s. For melting curve analysis, a dissociation step cycle (60°C for 10 s, and then 0.5°C for 10 s until 95°C) was added. For *LIP1*gene an initial activation step (95°C for 5 min) followed by 40 cycles of denaturation at 95°C for 15 s, annealing at 58°C for 30 s, and extension at 72°C for 30 s. For melting curve analysis, a dissociation step cycle (60°C for 10 s, and then 0.5°C for 10 s until 95°C) was added. For *CDR1* gene an initial activation step (95°C for 5 min) followed by 40 cycles of denaturation at 95°C for 15 s, annealing at 65°C for 30 s, and extension at 72°C for 30 s. For melting curve analysis, a dissociation step cycle (60°C for 10 s, and then 0.5°C for 10 s until 95°C) was added. For *Kex*2gene an initial activation step (95°C for 5 min) followed by 40 cycles of denaturation at 95°C for 15 s, annealing at 62°C for 30 s, and extension at 72°C for 30 s. For melting curve analysis, a dissociation step cycle (60°C for 10 s, and then 0.5°C for 10 s until 95°C) was added

Expression levels were quantified using relative quantization. All samples were analyzed in triplicate, and the ACT1 gene was used as an internal control housekeeping gene to normalize the levels of expression between samples. The real-time PCR data were analyzed by the (ΔΔCt) method [23, 24]. These values were normalized to *ACT1* expression as showed below:

$$\Delta Ct = Ct \text{ of tested gene} - Ct \text{ of housekeeping gene} \quad (1)$$

$$\Delta\Delta Ct = \Delta Ct \text{ (sample)} - \Delta Ct \text{ (calibrator)} \quad (2)$$

$$\text{Fold changes} = 2^{-\Delta\Delta Ct} \quad (3)$$

4. Statistical Analysis

The Statistical Analysis System- SAS program was used to detect the effect of difference factors in study parameters [25]. The data were analyzed for statistical significance using Chi-square test. P value less than 0.01 was considered significant. Also least significant difference – LSD-Test was used to significant compare between means in this study.

5. Results and Discussion

It was reported that plants extracts contain biomolecules including polyphenols, ascorbic acid, flavonoids, sterols,

triterpenes, alkaloids, alcoholic compounds, polysaccharides, saponins, β-phenylethylamines, glucose and fructose, and proteins/enzymes which could be used as reductant to react with silver ions and therefore used as scaffolds to direct the formation of AgNPs in the solution [26]. Tomato fruits were obtained at the light red stage of ripeness, because at this stage it contains all the components of the fruit, in addition to a proportion of chlorophyll. Silver ions act as electron acceptor species, the plant biomolecules acts as an electron donor species. Chlorophyll pigments act as a stabilizing agent between donor and acceptor molecule. The addition of tomato fruit extract at concentration of 10% at pH of 11 and to 2mM aqueous $AgNO_3$ at reaction temperature of 100°C changed the off White color of the solution to yellowish brown, which indicated the formation of AgNPs. Reduction of Ag^+ resulted in the color change from colorless to intense yellowish brown due to the formation of AgNPs which reflected bioreduction of Ag^+ to Ag°. The change in appearance seemed due to excitation of surface plasmon vibrations/ resonance in the AgNPs, depicted on the concentration of Ag ion revealed attachment of biomolecules forming the NPs and finally change in colour [27]. The plant extracts were reported to act as reducing and capping agents, thereby reducing the silver ions (Ag^+) to metallic silver (Ag°) [28]. The average particle size at pH11, tomato extract 10%, $AgNO_3$ 2*mM* and temperature of 100°C ranged from 9.58 to 72.69 nm. The particle size could be controlled by changing the reaction temperature, tomato fruit concentration, pH and $AgNO_3$ concentration.

Formation of the metal nanoparticles by reduction of the aqueous metal ions during exposure to tomato fruits extract may be easily followed by UV–Vis spectroscopy. It is observed that the silver surface plasma on resonance band centered at 340 nm. The absorption spectrum was recorded between 190 nm and 1100 nm. The spectrum of the sample was obtained for wavelength range and the band was noticed between 320-475 nm. This results were in agrement with the results of Gebru *et al*. (2013) who stated that metal nanoparticles exhibit weak absorbance around 300–400 nm, the absorption peak at 370 nm corresponds to the transverse plasmon vibration in the Ag nanoparticles (Figure 1).

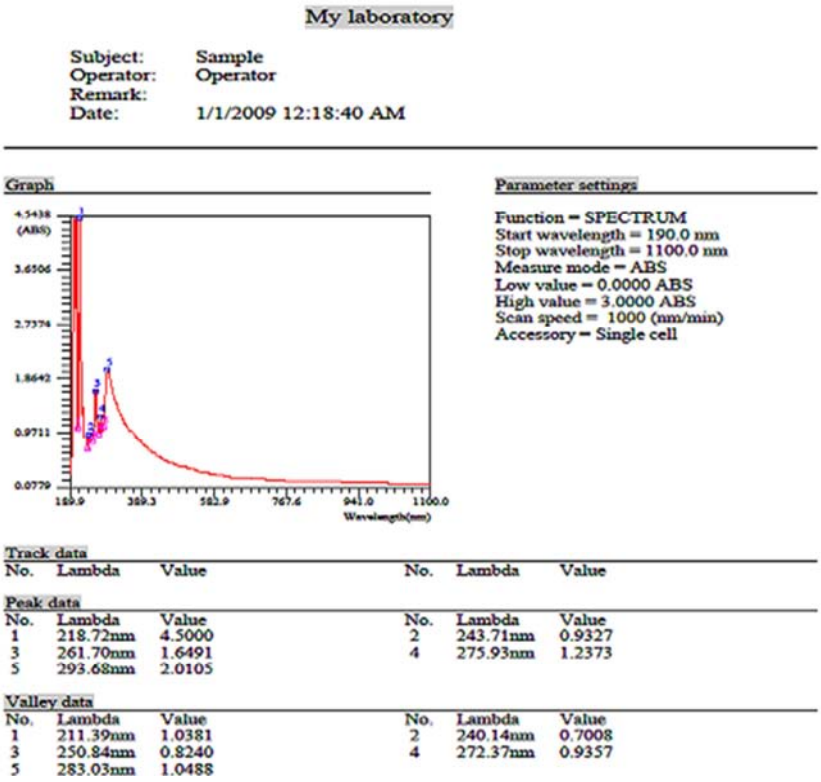

Figure 1. *UV-Vis absorption spectra of synthesized AgNPs by tomato fruites.*

FTIR measurements were performed over a range between 412.77 through 3822.91 cm^{-1}. The spectrum for tomato extract showed several peaks. The results of the FTIR spectroscopy of tomato extract and its AgNPs synthesized after the bioreduction are portrayed in Figure 2. The present study shows peak curves of the biosynthesized AgNPs from tomato extract resulted a strong bands at1936, 1882, 1803, 1764, 1656, 1602, 1510, 1392, 1222, 1188, 1085cm^{-1}. The band at 1936, 1882, 1803 and 1764 cm^{-1} was due to C=O stretching of the organic acid present in the extract. The bands at 1222 and 1188 cm^{-1} were linked to C-H stretching and O-H deformation of carboxyl groups. Large peaks 3822 through 3269cm^{-1} were corresponds to O–H stretching of carboxylic acids, and 2924cm^{-1} was (corresponds to the C–H stretching of alkane, aldehyde and alkene or aromatic [29]. Small peaks 600 cm^{-1} and less indicat the presence of C-Cl stretching of alkyl halides. [30]. The major content in flavonoids could reduce silver nitrate more successfully [31].

The XRD patterns obtained for the AgNPs showed a number of peaks at 25.3°, 42.5, 50.7°,, 54.0 and 76.8° in the 2θ range of 30°-90° which were pertained to (111), (200), (220), and (311) of AgNPs, respectively. The synthesis of silver nanoparticles at 100°C showed obvious clear peaks structure of silver at 111, 200, 220 and 311 (Figure 3). The diffraction peak of condition 100°C is sharp and higher than that synthesized at room temperature due to effect of the high temperature which made it easier to grow in a higher concentration of silver ion solution. Interestingly, most of researchers [27, 32, 33] that synthesized the nanoparticles using plant extracts seem to obtained a similar crystal structure.

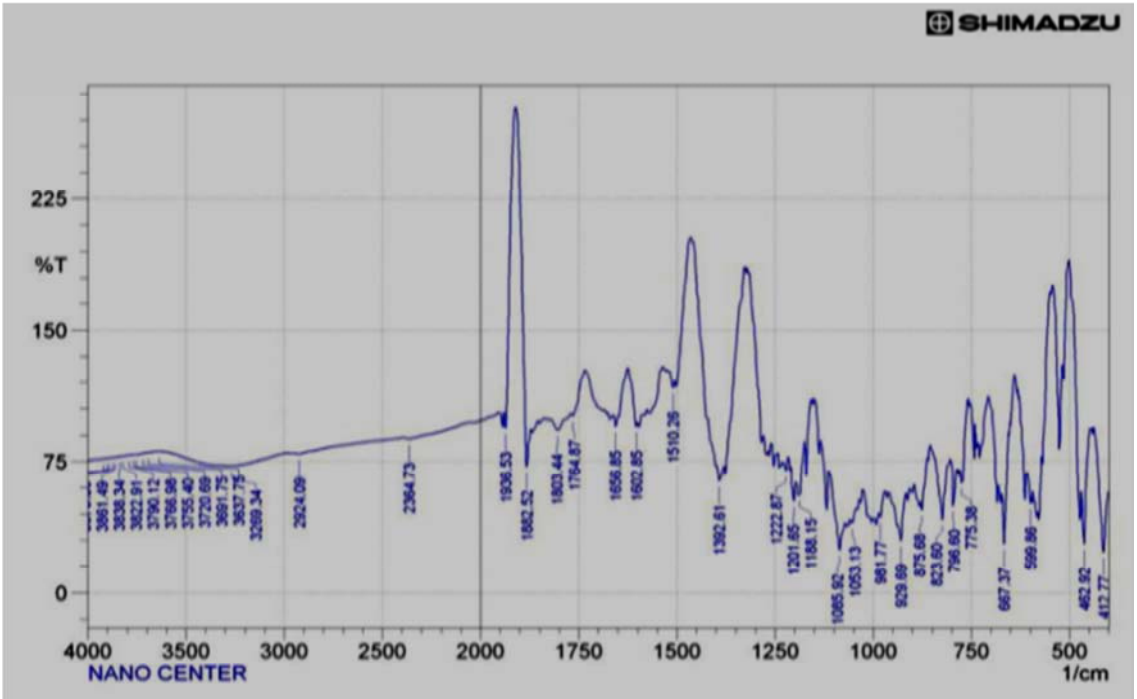

No.	Peak	Intensity	Corr. Intensity	Base (H)	Base (L)	Area	Corr. Area
1	412.77	23.13	48.23	437.84	399.26	11.46	6.35
2	462.92	27.79	36.05	468.7	449.41	4.79	1.96
3	599.86	51.07	11.64	607.58	594.08	3.29	0.54
4	667.37	27.85	34.38	671.23	640.37	3.9	1.84
5	775.38	62.85	15.17	779.24	759.95	1.75	0.83
6	796.6	49.61	24.66	804.32	785.03	3.58	0.99
7	823.6	41.77	34.89	854.47	810.1	8.67	3.98
8	875.68	47.26	10.62	879.54	864.11	3.46	0.49
9	929.69	29.64	24.53	948.98	918.12	11.8	3.44
10	981.77	43.05	5.88	985.62	970.19	4.56	0.28
11	1053.13	39.96	2.5	1055.06	1043.49	4.09	0.12
12	1085.92	24.2	25.6	1112.93	1072.42	15.82	4.33
13	1188.15	55.88	15.17	1195.87	1176.58	3.54	0.95
14	1201.65	52.45	14.03	1215.15	1197.79	3.57	0.8
15	1222.87	69.98	5.57	1226.73	1217.08	1.32	0.19
16	1392.61	63.93	8.52	1398.39	1381.03	2.92	0.48
17	1510.26	116.85	6.15	1519.91	1504.48	-1.29	0.13
18	1602.85	94.92	4.86	1625.99	1600.92	-1.23	-0.02
19	1656.85	95	6.33	1660.71	1649.14	0.09	0.15
20	1764.87	100.99	5.19	1770.65	1734.01	-1.77	0.31
21	1803.44	92.89	7.25	1820.8	1770.65	0.64	0.78
22	1882.52	72.2	73.82	1911.46	1870.95	-6.32	2.07
23	1936.53	94	32.22	1940.39	1911.46	-6.85	-0.26
24	2364.73	87.96	1.3	2391.73	2063.83	12.27	1.43
25	2924.09	79.36	1.38	2981.95	2393.66	44.26	0.64
26	3269.34	72.33	7.83	3593.38	2983.88	74.5	16.03
27	3637.75	80.71	0.12	3651.25	3624.25	2.5	0.01
28	3691.75	80.18	0.08	3695.61	3684.04	1.11	0
29	3720.69	79.63	0.04	3722.61	3695.61	2.62	0
30	3755.4	78.97	0.12	3759.26	3724.54	3.51	0.02
31	3766.98	78.85	0.14	3774.69	3761.19	1.39	0.01
32	3790.12	78.64	0.06	3792.05	3776.62	1.6	0
33	3822.91	78.04	0.19	3826.77	3793.98	3.48	0.02

Date/Time; 6/20/2019 9:26:42 AM

Figure 2. *FTIR spectrum of AgNPs with tomato fruits extract.*

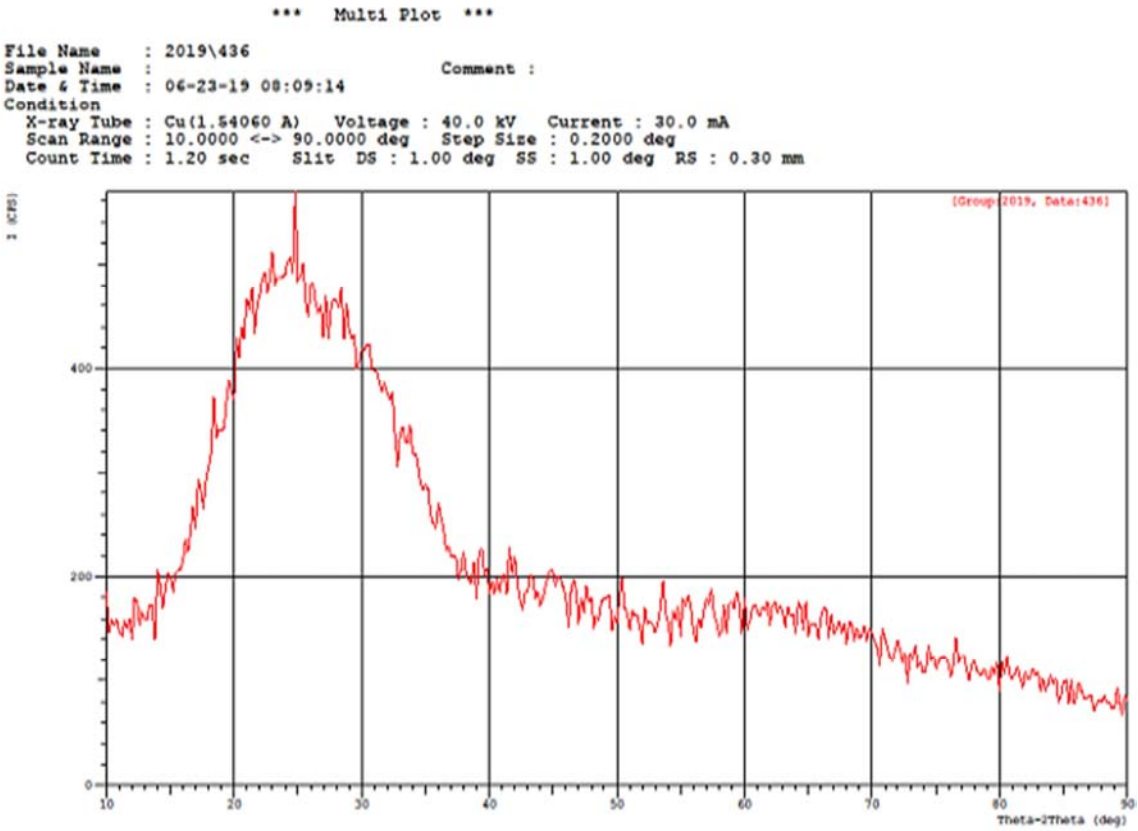

Figure 3. *XRD spectra of synthesis AgNPs.*

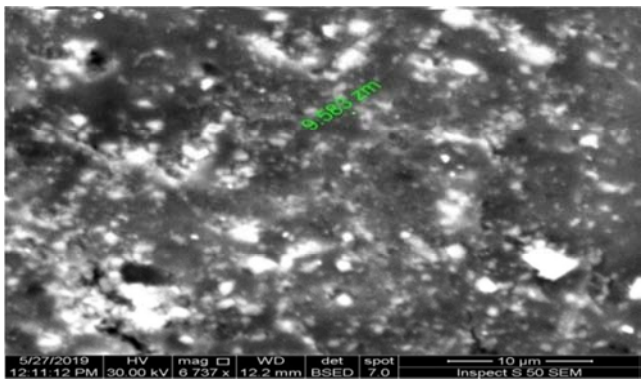

Figure 4. *SEM image of AgNPs synthesized from tomato fruits extract.*

Scanning electron microscope was employed to analyze the shape and size of the silver nanoparticles that were synthesized by the green method. The particle size distribution revealed that the average size of the obtained sample at pH11, tomato extract 10%, $AgNO_3$ 2*mM* and temperature of 100°C was approximately 9.58-72.69 nm. (Figure 4) and this result agreed with other researc [32, 34, 35].

6. Quantitative Real Time PCR (qPCR)

6.1. Real Time PCR Quantification of ACT1 Gene Expression

Real time PCR was used to determine the expression of virulence genes (*SAP1, CDR1, LIP1* and *KEX2*) in the cDNA samples, with *ACT1* gene used as a reference housekeeping gene to normalize the data. Many previous studies [20, 36, 37] used *ACT1*gene as housekeeping gene. No significant differences were found between control group and the groups treated with 15 and 20% AgNPs with respect to Ct for reference gene *ACT1 gene* which ranged from 23.87 to 23.91 (Table 2).

Table 2. *Comparison of ACT1 gene fold expression between studied groups.*

Groups	Means Ct of *ACT1*	2^{-Ct}	Experimental groups/ Control group	Fold of gene expression
AGNPs 20% (no.=10)	23.89	6.43 E-8	6.43 E-8/6.52 E-8	0.98±0.08
AgNPs 15% (no.=10)	23.91	6.34 E-8	6.34 E-8/6.52 E-8	0.97±0.05
LSD value	N. S	N. S	N. S	N. S
NS: Non-Significant.				

The assumption in the use of housekeeping genes in molecular studies is that their expression remains constant in the cells or tissue under investigation [38]. Freire *et al*. and Yu *et al*. studied the expression of *SAP1-5, LIP1, 4, 9, ALS1-3* and *PLB2* genes using qRT-PCR they applied the *ACT1* gene as a reference gene, and found that using of *ACT1* gene

is quite a reliable strategy for the normalization in qRT-PCR when applied in studies [36, 37]. Results of current study, recommend the use of the mean of the expression values from the housekeeping gene (*ACT1*) for normalization, when analyzing differences in gene expression levels between *C. albicans* isolates under different treatments. To further improvement, although there was no a significant difference in the mean Ct value between groups in the present study, the variation of total change in expression of *ACT1* gene was studied in different study groups utilizing the 2^{-Ct} value and the ratio of 2^{-Ct} of AgNPs treatments to control, as shown in Table 2. This table shown no differences between the concentration 15 and 20% of AgNP used in this study in 2^{-Ct} values were 6.34 and 6.43, and in fold of gene expression were 0.97and 0.98, respectively, renders that *ACT1* gene a useful control gene. The pattern of amplification of the gene was shown in the Figure 5 and its melting temperature ranged from 78°C to 84.23°C no primer dimer could be seen.

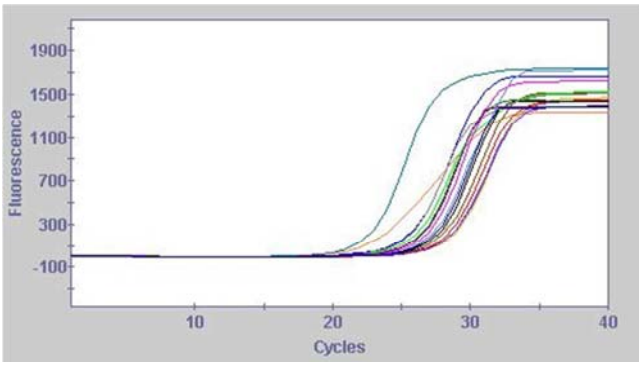

Figure 5. *ACT1 gene amplification plots by qPCR samples included all study treatments. Ct values ranged from 19-25. The photograph was taken directly from Cepheid (smart cycler) qPCR machine.*

6.2. Real Time PCR Quantification of SAP1 Expression

The quantification of gene expression was related to the production of hydrolytic enzymes using the quantitative polymerase chain reaction (qPCR) assay [36]. The results were obtained by comparison of the variation in Ct for the genes of interest in the treated groups and in the control group and are shown in Table 3. It is evident from these results that the control group is associated with the highest copy number of mRNAs reflecting its higher expression. These results showed a decrease in the expression of *SAP1* gene due to the damage caused by AgNPs on the genetic content. The tested groups exhibited different expression profiles after AgNPs, with a reduction in the expression of the *SAP1* gene. Comparing the gene expression between the control group (untreated) and the treated (concentration of 15 and 20%AgNPs) by statistical analysis (LSD test), it was observed that the AgNPs reduced the gene expression significantly (Figure 6). Given that fold change ranged from 0.22 to 0.15 (Table 3) it can be suggested that AgNPs succeeded in the suppression of *SAP1* gene expression. Its melting temperature ranged from 83°C to 86°C. Freire *et al*. (2015) reported that PDI (photosensitization with methylene blue followed by low-level laser irradiation) showed a slight reduction on the expression of hydrolytic enzymes (*SAP1*) of *C. albicans,* without statistical significance. The mechanism underlying the suppression of biofilm formation using AgNPs was reported to include the anti-adhesive action of AgNPs that regulate the growth of living microbial cells and the suppression of microbial adhesions gene expression [39]. In addition, AgNPs were shown to suppress blastospores and to disrupt the cell wall of both the yeast and the filamentous forms in order to cause the inhibition of biofilm formation in Candida [40]. Ali and Abdallah [41] demonstrated that the efficiency of the antifungal activity of AgNPs could be enhanced via the combination therapy of AgNPs with natural antifungal agents to provide a novel strategy for the efficient control of *C. albicans*.

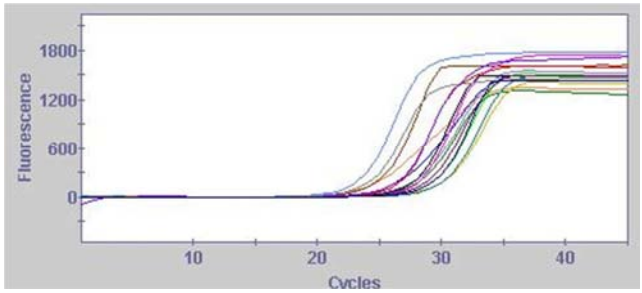

Figure 6. *SAP1 gene amplification plots by qPCR samples included all study groups. Ct values ranged from 20-26. The photograph was taken directly from cephied (smart cycler) qPCR machine.*

Table 3. *Fold of SAP1 gene expression depending on $2^{-\Delta\Delta Ct}$ Method.*

Groups	Means Ct of *SAP1*	Means Ct of *ACT1*	Mean ΔCt Target (Ct*SAP1*-Ct *ACT1)*	Mean ΔCt Calibrator (Ct*SAP1*-Ct *ACT1*	ΔΔCt	$2^{-\Delta\Delta Ct}$	experimental group/ Control group	Fold of gene expression
AgNPs20% (no.=10)	25.96	23.89	2.07	0.69	1.38	0.38	0.38/2.46	0.15±0.06
AgNPs 15% (no.=10)	25.44	23.91	1.53	0.69	0.84	0.55	0.55/2.46	0.22±0.08
Control (no.=10)	23.26	23.87	-0.61	0.69	-1.3	2.46	2.46/2.46	1.00±0.00
LSD vvalue								0 0.407**

** (P≤0.01).

6.3. Real Time PCR Quantification of LIP1 Expression

The present assay represents a trial to search for new antifungal agents. AgNPs possessed high antimicrobial activity which was tested against *C. albicans* that was isolated in the present survey from patients. The application of genome- expression profiling to determine how drugs achieve their therapeutic effect, used mRNA to identify lipase gene of *C. albicans* whose expression is changed after treatment with AgNPs act as anti-fungal drug. Suppressing of

expressed lipase gene in treated sample than untreated one refers to the effect of AgNPs on lipase gene that illustrated its inhibitory effect on lipase enzyme activity (Figure 7). Table 4 showed that AgNPs at concentrations of 15 and 20%, had effect on the ratio of lipase gene expression that quantified by real-time PCR, by comparing of fold values which were 0.61 and 0.66, respectively of amplified cDNA extracted from *C albicans* treated with AgNPs with those obtained from untreated *C albicans*. The melting temperature (*Tm*) value obtained was in range 81-83°C. The secretion of hydrolytic enzymes is reported to play an important role in the pathogenicity of *Candida*. The adhesions, lipases and Saps are encoded by *LIP* and *SAP* genes (*SAPT1-4*), respectively [42]. Metwally *et al*. [43] stated that lipase gene expression was reduced by *Pluchea dioscoridis* leaf extract from 100% to 7% and 19% than that obtained from untreated *A. niger* as documented by quantitative RT-PCR analysis, and consequently the lipase enzyme activity that play a role in the pathogenecity of *A. niger* in otomycosis infection.

Table 4. *Fold of LIP1gene expression depending on $2^{-\Delta\Delta Ct}$ Method.*

Groups	Means Ct of *LIP1*	Means Ct of *ACT1*	Mean ΔCt Target (Ct*LIP1*-Ct *ACT1)*	Mean ΔCt Calibrator (Ct*LIP1*-Ct *ACT1*)	ΔΔCt	$2^{-\Delta\Delta Ct}$	experimental group/ Control group	Fold of gene expression
AgNPs 20% (no.=10)	24.45	23.89	0.33	1.33	-1	2	2/3.01	0.66±0.05
AgNPs 15% (no.=10)	24.65	23.91	0.44	1.33	-0.89	1.85	1.85/3.01	0.61±0.05
Control (no.=10)	23.89	23.87	-0.26	1.33	-1.59	3.01	3.01/30.1	1.00±0.00
LSD value								0.297 *
* (P≤0.05).								

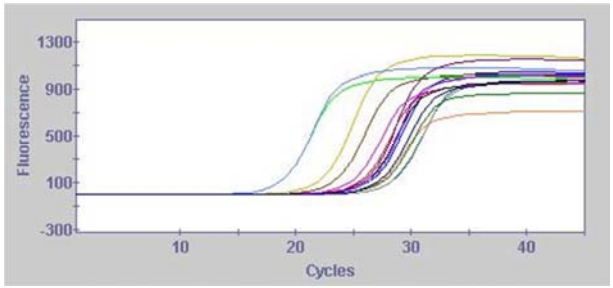

Figure 7. *LIP1 gene amplification plots by qPCR samples included all study groups. Ct values ranged from 16-26. The photograph was taken directly from Cepheid (smart cycler) qPCR machine.*

6.4. Real Time PCR Quantification of CDR1 Expression

To evaluate the expression of the CDR1 gene in *C. albicans* after AgNPs, enzymes that play an important role in the virulence of this yeast has been one of the subject in this study. The experiment was done in order to determine if altering AgNPs doses alters the gene induction response in Candida albicans. Reverse transcription PCR (RT-PCR) analysis revealed the overexpression (Fgure 8) While previous works have shown that there are overexpressed [44, 45] the results of the current study was confirmed the results of those studies and showed significant overexpression with fold of 5.81 and 4.69 with increasing AgNPs concentrations to 15 and 20%, respectively (Table 5). The melting temperature (*Tm*) value obtained was in range 82-84°C. Efflux pumps *CDR1*, *CDR2* and the multidrug resistance transporter *MDR1* have shown to be overexpressed in the resistant clinical isolates (White 1997). Monroy-Pérez *et al*. (2016) used in vitro model of infection with *C. albicans*, the clinical strains showed different expression profiles of virulence genes in association with the azole resistance gene *CDR1*, and concluded that the strains all are insensitive to azoles. Khanna [45] reported that in the presence of fluconazole (FLC) drug, the expression levels changed the levels of *CDR1*was the highest at 4 µg/ml to 256 µg/ml. Hence, at concentrations below its MIC80 (<256 µg/ml), FLC did not have a significant effect on gene induction. In this study it appears that it needs higher concentrations of AgNPs to inhibit its gene expression.

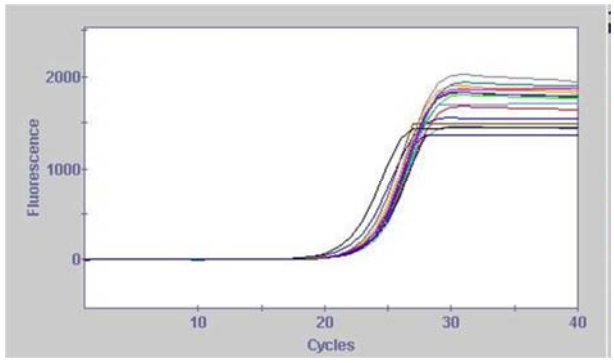

Figure 8. *CDR1 gene amplification plots by qPCR samples included all study groups. Ct values ranged from 19-25. The photograph was taken directly from Cepheid (smart cycler) qPCR machine.*

Table 5. *Fold of CDR1 gene expression depending on $2^{-\Delta\Delta Ct}$ Method.*

Groups	Means Ct of *CDR*1	Means Ct of *ACT1*	Mean ΔCt Target (Ct*CDR1*-Ct*ACT1)*	Mean ΔCt Calibrator (Ct*CDR1*-Ct*ACT1*	ΔΔCt	$2^{-\Delta\Delta Ct}$	experimental group/ Control group	Fold of gene expression
AgNPs 20% (no.=10)	20.39	23.89	-3.73	3.11	-6.84	114.56	114.56/24.42	4.69±0.17
AgNPs 15% (no.=10)	20.17	23.91	-4.04	3.11	-7.15	142.02	142.02/142.02	5.81±0.25
Control (no.=10)	22.65	23.87	-1.5	3.11	-4.61	24.42	24.42/24.42	1.00±0.00
LSD value								1.253 **
** (P≤0.01)								

6.5. Real Time PCR Quantification of KEX2 Expression

The expression of *Kex2* gene in *C. albicans* was quantified by RT-qPCR. The data in Figure 9 revealed that the AgNPs at concentration of 20%, downed expression significantly the expression level of this gene, with fold of 0.84 (Table 6). Melting temperature of this gene ranged from 82°C to 84°C. While AgNPs at concentration of 15% not affect on the expression of *Kex2* gene. It appears that this gene requires higher concentrations of AgNPs, similar to a gene *CDR1*. Inactivation of the *kexin* (*KEX2*) gene results in a marked attenuation in *C. albicans* virulence due partly to a defect in the expression of two major virulence factors: the secretion of active aspartyl proteinases and the formation of hyphae [46], govern the efficiency of exit from phagocytic cells [47]. Disruption of *Kex2* gene function in *C. albicans* has pleiotropic effects that may impinge on the ability of the organism to colonize and invade tissues [48].

Table 6. *Fold of Kex2 gene expression depending on $2^{-\Delta\Delta Ct}$ Method.*

Groups	Means Ct of *Kex2*	Means Ct of *ACT1*	Mean ΔCt Target (Ct*Kex2*-Ct*ACT1*)	Mean ΔCt Calibrator (Ct*Kex2*-Ct*ACT1*	ΔΔCt	2-ΔΔCt	Experimental group/ Control group	Fold of gene expression
AgNPs 20% (no.=10)	21.916	23.89	-2.204	-0.7	-1.28	2.42	2.42/2.88	0.84±0.07
AgNPs 15% (no.=10)	21.658	23.91	-2.552	-0.7	-1.56	2.94	2.94/2.88	1.02±0.11
Control (no.=10)	21.646	23.87	-2.504	-0.7	-1.53	2.88	2.88/2.88	1.00±0.00
LSD value	-	-	-	-	-	-	-	0.135 *

* (P≤0.05).

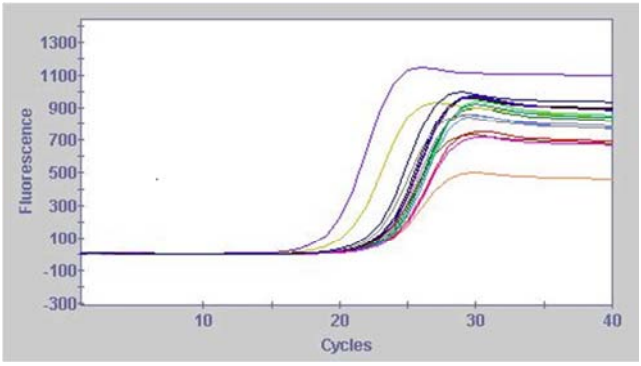

Figure 9. *Kex2 gene amplification plots by qPCR samples included all study groups. Ct values ranged from 18- 25. The photograph was taken directly from Cepheid (smart cycler) qPCR machine*

7. Conclusion

Virulence factors are very important determinants of any microorganism that help to differentiate pathogenic from non pathogenic species. The presence of virulence factors in *C. albicans* isolates may give the signal of invasiveness of the *candida* species. Changes in *Sap1, LIP1* and *Kex2* genes expression may attribute to become fungi unable to cause infection. Thus, AgNPs provides a novel strategy for preventing the pathogenesis of *C. albicans* by suppressing the key virulence factors and development of biofilms. But AgNPs concentrations used in this study could not suppress the expression of the *CDR1* gene, and it appears that it requires higher concentrations to be used to suppressing it.

References

[1] Ali, E. M. and Abdallah, B. M. (2020). Effective inhibition of Candidiasis using an eco-friendly leaf extract of *Calotropis-gigantean*-mediated silver nanoparticles. Nanomaterials, 10: 422, 16 pages.

[2] Ananda, D.; Babu, S. T. V.; Joshi, C. G. and Shantaram, M. (2015). Synthesis of gold and silver nanoparticles from fermented and non fermented betel leaf. Int. J. Nanomater. Bios., 5: 20–23.

[3] Calderone, R. A. and Clancy, C. J. (2012). Candidaand Candidiasi. Second Edition. ASM Press: Washington, D. C.

[4] Canteri de Souza, P.; Custódio Caloni, C.; Wilson, D. and Sergio Almeida, R. (2018). An invertebrate host to study fungal infections, Mycotoxins and Antifungal Drugs. J. Fungi (Basel), 4: 125.

[5] Correia, A.; Lermann, U.; Teixeira, L.; Cerca, F.; Botelho, S.; da Costa, R. M. G. *et al*. (2010). Limited role of secreted aspartyl proteinases *Sap1* to *Sap6* in *Candida albicans* virulence and host immune response in murine hematogenously disseminated Candidiasis. Infection and Immunity, 78 (11): 4839–4849.

[6] Dakal, T. C.; Kumar, A.; Majumdar, R. S. and Yadav, V. (2016). Mechanistic basis of antimicrobial actions of silver nanoparticles. Front. Microbiol., 7: 1831, 47 pages.

[7] Das, I.; Parida, U. K. and Bindhani, B. K. (2014). Synthesis of plant- mediated silver nanoparticles using *Lycopersicon esculentum* L. extract and evaluation of their antimicrobial activities. Int. J. Pharm. Bio. Sci., 5 (3): 307–322.

[8] Flowers, S. A.; Barker, K. S.; Berkow, E. L.; Toner, G.; Chadwick, S.; Gygax, S. E. *et al*. (2012). Gain-of-function mutations in UPC2 are a frequent cause of ERG11 upregulation in azole-resistant clinical isolates of Candida albicans. Eukaryotic cell, 11 (10): 1289-1299.

[9] Freire, F.; de Barros, P. P.; Ávila, D. S.; Back Brito, G. N.; Junqueira, J. C. and Jorge, A. O. C. (2015). Evaluation of gene expression *SAP5, LIP9*, and *PLB2* of *Candida albicans* biofilms after photodynamic inactivation. Lasers Med. Sci., 30: 1511–1518.

[10] Gebru, H.; Taddesse, A.; Kaushal, J. and Yadav, O. P. (2013). Green synthesis of silver nanoparticles and their antibacterial activity. J. Surface Sci. Technol., 29 (1-2): 47-66.

[11] Ghosh, S.; Patil, S.; Ahire, M.; Kitture, R.; Gurav, D. D.; Jabgunde, A. M. *et al.* (2012). *Gnidia glauca* flower extract mediated synthesis of gold nanoparticles and evaluation of its chemocatalytic potential. J. Nanobiotechnology, 10: 17.

[12] Gulati, M. and Nobile, C. J. (2016). *Candida albicans* biofilms: Development, regulation, and molecular mechanisms. Microbes Infect, 18: 310–321.

[13] Halbandge, S. D.; Mortale, S. P. and Karuppayil, S. M. (2017). Biofabricated silver nanoparticles synergistically activate amphotericin B against mature biofilm forms of *Candida albicans*. The Open Nanomedicine Journal, 4: 1-16.

[14] Husen, A. and Siddiqi, K. S. (2014) Phytosynthesis of nanoparticles: concept, controversy and application. Nanoscale Res. Lett., 9: 229–252.

[15] Iyalla, C. (2017). A review of the virulence factors of pathogenic fungi. African Journal of Clinical and Experimental Microbiology, 18 (1): 53-58.

[16] Khan, N. T. and Mushtaq, M. (2018). Determination of antifungal activity of silver nanoparticles produced from *Aspergillus niger*. Biology and Medicine, 9 (1): 1000363, 4 pages.

[17] Khanna, A. (2015). Expression Pattern of Drug-Resistance Genes in *Candida Albicans* at Different Fluconazole Concentrations. MS. c. Thesis. Faculty of the University of Missouri-Kansas. USA.

[18] Köhler, J. R.; Casadevall, A. and Perfect, J. (2015). The spectrum of fungi that infects humans. Cold Spring Harb. Perspect. Med., 5 (1): a019273, 57 pages.

[19] Lamoth, F. and Kontoyiannis, D. P. (2018). The Candida auris alert: Facts and perspectives. The Journal of infectious diseases, 217 (4): 516–520.

[20] Livak, K. J. and Schmittgen, T. D. (2001). Analysis of relative gene expression data using real-time quantitative PCR and the $2^{-\Delta\Delta ct}$ method. Methods, 25: 402-408.

[21] Lo, H. J.; Kohler, J. R.; DiDomenico, B.; Loebenberg, D.; Cacciapuoti, A., and Fink, G. R. (1997). Nonfilamentous *C. albicans* mutants are avirulent. Cell, 90: 939–949.

[22] Many, J. N.; Radhika, B. and Ganesan, T. (2014). Synthesis of silver nanoparticles using fresh tomato pomace extract. International Journal of Nanomaterials and Biostructures, 4 (1): 12-15.

[23] Metwally, M. A.; Gamea, A. M.; Hafez, E. E. and El Zawawy, N. A. (2015). A Survey on the effect of ethanol *Pluchea dioscoridis* leaf extract on lipase gene expression in otomycotic *Aspergillus niger* via Real-time PCR. International Journal of Advanced Research, 3 (5): 1197-1206.

[24] Monroy-Pérez, E.; Paniagua-Contreras, G. L.; Rodríguez-Purata, P.; Vaca-Paniagua, F.; Vázquez-Villaseñor, M.; Díaz-Velásquez, C. *et al*. (2016). High virulence and antifungal resistance in clinical strains of *Candida albicans*. Canadian Journal of Infectious Diseases and Medical Microbiology, 2016: 5930489, 7 pages.

[25] Moteriya, P. and Chanda, S. (2018). Biosynthesis of silver nanoparticles formation from *Caesalpinia pulcherrima* stem metabolites and their broad spectrum biological activities. Journal of Genetic Engineering and Biotechnology, 16: 105–113.

[26] Nailis, H.; Kucharikova, S.; Ricicova, M.; Van Dijck, P.; Deforce, D.; Nelis, H. *et al*. (2010). Real-time PCR expression profiling of genes encoding potential virulencefig factors in *Candida albicans* biofilms: identification of model-dependent and - independent geneexpression. BMC Microbiology, 10: 114.

[27] Newport, G. and Agabian, N. (1997). KEX2 influences *Candida albicans* proteinase secretion and hyphal formation. J. Biol. Chem., 272: 28954–28961.

[28] Newport, G.; Kuo, A.; Flattery, A.; Gill, C.; Blake, J. J.; Kurtz, M. B. *et al.* (2003). Inactivation of Kex2p diminishes the virulence of *Candida albicans*. The Journal of Biological Chemistry, 278 (3): 1713–1720.

[29] Obiazikwor, O. H. and Shittu, H. O. (2018). Antifungal activity of silver nanoparticles synthesized using *Citrus sinensis* peel extract against fungal phytopathogens isolated from diseased tomato (*Solanum lycopersicum* L.). Issues in Biological Sciences and Pharmaceutical Research, 6 (3): 30-38.

[30] Prasad, R. (2014). Synthesis of silver nanoparticles in photosynthetic plants. Journal of Nanoparticles, 2014: 963961, 8page.

[31] Rai, A.; Prabhune, A. and Perry, C. C. (2010). Antibiotic mediated synthesis of gold nanoparticles with potent antimicrobial activity and their application in antimicrobial coatings. J. Mater. Chem., 20: 6789-6798.

[32] Rajoriya, P. (2017). Green Synthesis of Silver Nanoparticles, their Characterization and Antimicrobial Potential. Ph. D. Thesis. Jacob Institute of Biotechnology and Bioengineering, Sam Higginbottom University of Agriculture, Technology and Sciences, India.

[33] Rajput, K.; Raghuvanshi, S.; Bhatt, A.; Rai, S. K. and Agrawal, P. K. (2017). A review on synthesis silver nano-particles. Int. J. Curr. Microbiol. App. Sci., 6 (7): 1513-1528.

[34] Reboucas E.; Costa J.; Passos M.; Passos J.; Hurk R. and Silva J. (2013). Real time PCR and importance of housekeepings genes for normalization andquantification of mRNA expression in different tissues. Brazilian Archives of Biology and Technology, 56: 143-154.

[35] Reidy, B.; Haase, A.; Luch, A.; Dawson K. A. and Lynch, I. (2013). Mechanisms of silver nanoparticle release, transformation and toxicity: A critical review of current knowledge and recommendations for future studies and applications. Materials, 6: 2295-2350.

[36] Renugadevi, T. S.; Gayathri, S. (2010). FTIR and FT-Raman spectral analysis of paclitaxel drugs. Int. J. Pharm. Sci. Rev. Res., 2 (2): 106–110.

[37] Rodríguez-Luis, O. E.; Hernandez-Delgadillo, R.; Sánchez-Nájera, R. I.; Martínez-Castañón, G. A.; Niño-Martínez, N.; Navarro, M. C. S. *et al*. (2016). Green synthesis of silver nanoparticles and their bactericidal and antimycotic activities against oral microbes Journal of Nanomaterials, 2016: ID 9204573, 10 pages.

[38] Roy, A.; Bulut, O.; Some, S.; Mandal, A. K. and Yilmaz, M. D. (2019). Green synthesis of silver nanoparticles: biomolecule- nanoparticle organizations targeting antimicrobial activity. The Royal Society of Chemistry Advances, 9: 2673–2702.

[39] Ryder, M. A. (2005). Catheter - related infections: It's all about biofilm. Advanced Practice Nursing e J., 5 (3): 1-15.

[40] Rozalska, B.; Sadowska, B.; Budzynska, A.; Bernat, P. and Rozalska, S. (2018). Biogenic nanosilver synthesized in *Metarhizium robertsii* waste mycelium extract—As a modulator of *Candida albicans* morphogenesis, membrane lipidome and biofilm. PLoS One, 13: e0194254.

[41] Salari, S.; Bahabadi, S. E.; Samzadeh-Kermani, A. and Yosefzaei, F. (2019). *In-vitro* evaluation of antioxidant and antibacterial potential of green synthesized silver nanoparticles using *Prosopis farcta* fruit extract. Iranian Journal of Pharmaceutical Research, 18 (1): 430-445.

[42] Salati, S.; Doudi, M. And Madani, M. (2018). The biological synthesis of silver nanoparticles by mango plant extract and its anti-*Candida* effects. Journal of Applied Biotechnology Reports, 5 (4): 157-161.

[43] SAS. (2012). Statistical Analusis, User's Guide. Statistical Version9. 1th ed. SAS. Inst. Inc. Cary. N. C. USA.

[44] Silva, S.; Negri, M.; Henriques, M.; Oliveira, R.; Williams, D. W. and Azeredo, J. (2011). Adherence and biofilm formation of non-*Candida albicans Candida* species. *TrendsMicrobiol.* 19, 241–247.

[45] White, T. C. (1997). Increased mRNA levels of *ERG16, CDR*, and *MDR1* correlate with increases in azole resistance in *Candida albicans* isolates from a patient infected with human immunodeficiency virus. Antimicrob Agents Chemother, 41 (7): 1482-1487.

[46] Yu, S.; Li, W.; Liu, X.; Che, J.; Wu, Y. and Lu, J. (2016). Distinct expression levels of *ALS, LIP*, and *SAP* genes in *Candida tropicalis* with diverse virulent activities. Front. Microbiol., 7: 1175, 10 pages.

[47] Zhang, X-F.; Liu, Z-G.; Shen, W. and Gurunathan, S. (2016). Silver nanoparticles: Synthesis, characterization, properties, applications, and therapeutic approaches. Int. J. Mol. Sci., 17: 1534-1568.

[48] Zia, M.; Gu, S.; Akhtar, J.; ul Haq, I.; Abbasi, B. H.; Hussain, A. *et al*. (2016). Green synthesis of silver nanoparticles from grape and tomato juices and evaluation of biological activities. The Institution of Engineering and Technology, IET Nanobiotechnology, 2015: 0099, 7 pages.